NASA TECHNICAL MEMORANDUM

NASA TM X-68143

NASA TM X-68143

POPULATION INVERSION CALCULATIONS USING NEAR RESONANT CHARGE EXCHANGE AS A PUMPING MECHANISM

by Donald L. Chubb and James R. Rose
Lewis Research Center
Cleveland, Ohio

TECHNICAL PAPER proposed for presentation at
Twenty-fifth Annual Gaseous Electronics Conference
London, Ontario, October 17-20, 1972

POPULATION INVERSION CALCULATIONS USING NEAR RESONANT CHARGE EXCHANGE AS A PUMPING MECHANISM

by Donald L. Chubb and James R. Rose
Lewis Research Center

ABSTRACT

Near resonance charge exchange between ions of a large ionization potential gas such as helium or neon and vapors of metals such as zinc, cadmium, selenium, or tellurium has produced laser action in the metal ion gas. The present investigation is a theoretical study of the possibility of obtaining population inversions in near resonant charge exchange systems (Xe-Ca, Xe-Mg, Xe-Sr, Xe-Ba, Ar-Mg, N-Ca). The analysis is an initial value problem that utilizes rate equations for the densities of relevant levels of the laser gas (Ca, Ba, Mg, or Sr) and an electron energy equation. Electron excitation rates are calculated using the Bohr-Thomson approximation for the cross section. Approximations to experimental values of the electron ionization cross section and the ion-atom charge exchange cross section are used. Preliminary results have been obtained for the Ca-Xe system and show that it is possible to obtain gains greater than 10^{14} m^{-3} with inversion times up to 8×10^{-7} second. A possible charge exchange laser system using a MPD arc plasma accelerator is also described.

E-7162

I. INTRODUCTION

McGowan and Stebbings (ref. 1) proposed that near-resonance charge exchange is a possible way of obtaining an inversion in a gas laser. Experimentally it was found that charge exchange was a pumping mechanism for producing inversions in He-Zn (refs. 2, 3, and 4), He-Cd (ref. 5), He-Se (refs. 6 and 7), He-Te (ref. 8), and Ne-Te (ref. 8). Theoretically there are many systems where near-resonance charge exchange can be used to produce an inversion.

The present theoretical study investigates the possibility of obtaining inversions in a plasma of metals such as Mg, Ca, Sr, or Ba by charge exchange with inert gas ions such as He, Ne, Xe, Ar, or N. The analysis uses rate equations to calculate the density of the various ion levels considered and an energy equation to calculate the electron temperature. Both charge exchange and electron collisional excitation of the various ion levels are considered.

In the next section a charge exchange laser system is described. Following that the analysis is presented. Then the important collision cross sections are discussed. Finally results of the analysis for the Ca-Xe system are discussed and conclusions are drawn.

II. CHARGE EXCHANGE ION LASER

Near resonance charge exchange is described by the following reaction.

$$A^+ + B \xrightarrow{\ell^i_{A0}} A + B_i^+ + \Delta E \qquad (1a)$$

The excited ion, B_i^+, corresponds to the upper laser level of the metal being considered. The ground state ion, A^+, corresponds to the inert gas ion. The quantity ℓ^i_{A0} is the excitation rate for the B_i^+ state by charge exchange with A^+. The quantity ΔE is given by

$$E = I.P._A - \left(I.P._B + E.P._{B_i^+}\right) \qquad (1b)$$

where I.P. is ionization potential E.P. is excitation potential. If ΔE is small, then the reaction rate, ℓ^i_{A0}, for this process will be comparable to the resonance process where $\Delta E \equiv 0$. Such charge exchange rates are large compared to electron and radiative excitation rates and therefore make it possible to preferentially excite the $(B^+)_i$ state. There are many possible choices for A and B that satisfy the requirement $\Delta E \to 0$. It is a reaction of the type described by equation (1a) that produced inversions in the experiments of references 2 to 8.

Table I lists some interesting possible systems. The first column lists the charge exchange reaction that populates the upper laser level of the metal ion. Column two lists the possible laser transition and column three gives the laser wavelength (ref. 18). The fourth column gives the value of the energy defect, ΔE, and the last column is the upper bound on the efficiency of the system. This efficiency is defined as the ratio of the energy of the laser photon, hc/λ, to the ionization potential of the inert gas, I.P. (species A in eq. (1a)).

In addition to the charge exchange reaction of equation (1a), the following charge exchange reaction may also produce inversions.

$$A + B^+ \xrightarrow{\ell^i_{AB^+}} A^+ + B_i + \Delta E \qquad (2a)$$

Here,

$$E = I.P._B - (I.P._A + E.P._{B_i}) \qquad (2b)$$

Again there are many systems where $\Delta E \to 0$ so that a large reaction rate can be expected.

Referring to equation (1b) we see that the A species must have a large ionization potential (for example, an inert gas) in order that $\Delta E \rightarrow 0$ and equation (1a) be a near resonant reaction. For equation (2a) to be a near resonant reaction, however, the A species must have a small ionization potential (for example, a metal).

Previous laser action based on equation (1a) has been obtained in discharge tubes running on He or Ne seeded with a metal (refs. 2 to 8). Inherently such devices establish plasma conditions (electron temperature and density) necessary to maintain the discharge. Usually these same conditions are not proper for obtaining large gains. Hopefully, as power is increased to the discharge the gain should increase. However, as power is increased the gain increases to a maximum and then decreases (ref. 7). The reason for the decrease in gain with increasing power is that the electron temperature increases with power and finally becomes large enough so that electron collisions drive all the excited states toward their equilibrium values thus eliminating the inversion.

The ideal system for a charge exchange laser would be one where the plasma conditions for obtaining gain are independent of those necessary for maintaining the source of ions. One device that has the possibility of providing this independent control is a plasma accelerator called an MPD arc (refs. 9 and 10). The MPD arc produces a stream of high velocity (1.5×10^4 m/sec) ions at densities up to 10^{20} m^{-3} (ref. 11). A proposed system for obtaining gain using charge exchange with an MPD arc is illustrated in figure 1. A seed metal is added to the exhaust of the arc. An inversion in the metal ion gas should be produced by means of the charge exchange reaction described by equation (1a). Since the seed metal is located downstream of the arc discharge, it will not seriously alter the discharge operation. Therefore, the amount of metal seed that can be added will be nearly independent of the arc operation. Also, although the electron temperature in the arc exhaust is determined by the discharge conditions, it decreases with distance downstream from the active arc plume. As a result, by choosing the point at which the metal seed is added the electron temperature that effects the gain can be controlled. An additional advantage of the MPD arc system is that it can be run at high powers (megawatts) so that large gains may be possible.

An MPD arc system similar to that shown in figure 1 is being constructed. To estimate the possible gains that may be obtained a theoretical analysis was initiated. The following model was used to approximate the conditions that exist in figure 1. A beam of inert gas ions is assumed to be moving through a cloud of neutral ground state metal gas. Initially the ion beam and metal gas cloud have prescribed spatially uniform densities. Then treating this situation as an initial value problem, the densities of the important states are calculated as functions of time. The electron temperature is also calculated as a function of time. Conditions that exist in the initial penetration of the ion beam into the metal gas cloud should be approximated by this model. Results of this analysis will indicate the magnitude of the inversion, as well as the length of time the inversion will persist in the initial interaction of the ion beam and metal gas cloud.

III. ANALYSIS

To obtain an exact solution for all the number densities of the excited states of the metal ion would require solving the continuity, momentum, and energy equations for each of the excited states of the metal. Also, similar equations for all states of the inert gas and electron gas must be included. Such a problem would be intractable. However, several simplifications can be made. First of all, only a limited number of levels of the metal ion will be important in determining an inversion. As a result, most of the excited states can be neglected. Secondly, since elastic collision rates between like species are large, we can represent all states of the metal by a common temperature and velocity. Thirdly, the characteristic time for a change in density of an excited metal ion state is short (10^{-8} sec) compared to the momentum transfer collision time (10^{-6} sec) between the inert gas ions and the metal. As a result we assume that the velocity and temperature of the inert gas ions and the velocity and temperature of all the metal states are constants. Finally, heat conduction and viscous dissipation are neglected. With these approximations the system of equations to be solved includes a continuity equation for each considered state of the metal, the electron continuity equation, the inert ion continuity equation, and an electron energy equation.

A. Continuity Equation for i^{th} Level of Metal Ion

The continuity equation for the i^{th} level is given by the following expression (ref. 12, ch. 7-8).

$$\frac{\partial n_i}{\partial t} + \nabla \cdot (n_i \vec{v}_i) = P_A^i + P_e^i + P_{rad}^i \tag{3}$$

where $\vec{v}_i$ is the average velocity and n_i is the number density of the i^{th} species and t is time. The P terms on the right hand side of equation (3) give the production rate of the i^{th} species as a result of charge exchange P_A^i, collisional electron excitation P_e^i, and spontaneous emission and stimulated emission and absorption P_{rad}^i. In appendix A expressions for these terms are developed. In considering the charge exchange production term we neglected the inverse deexcitation process (see eq. (1a)). This is reasonable since the densities of the inert gas atom and excited metal ion are small compared to the inert gas ion and ground state metal atom. It was assumed that the radiation field used to calculate the stimulated emission and absorption effects is not dependent on the densities of the excited levels of the metal ion. Instead the radiation energy flux was assumed to have a Planck distribution in frequency and to be characterized by some radiation temperature, T_r, and a parameter, γ, that accounts for an increase in energy flux at any frequency where lasing may occur (see appendix A). Since we have assumed $\vec{v}_i$ is nearly constant for time intervals of interest, equation (3) becomes the following.

$$\frac{\partial n_i}{\partial t} + \vec{v}_i \cdot \nabla n_i \equiv \frac{dn_i}{dt} = P_A^i + P_e^i + P_{rad}^i \tag{4}$$

B. Continuity Equation for Metal Ion Ground State

For the ground state of the metal ion, an additional term must be added to equation (4) that accounts for ionization of neutral metal atoms by electron impact. Therefore,

$$\frac{dn_1}{dt} = P_e^1 + P_{rad}^1 + n_o n_e \ell_{eo}^1 - n_e^2 n_1 k_{el}^o \tag{5}$$

Where subscript or superscript 1 denotes the ground state of the ion and subscript or superscript o denotes the ground state of the neutral metal atom. Note that ℓ_{eo}^1 and k_{el}^o are ionization and recombination rates. Similar to the case of electron excitation (eq. (A7)) we relate the recombination rate, k_{el}^o, to the ionization rate, ℓ_{eo}^1, through the equilibrium relation (ref. 13, p. 687)

$$k_{el}^o = \frac{1}{2}\frac{g_0}{g_1}\left(\frac{h^2}{2\pi m_e kTe}\right)^{3/2} e^{\frac{qE_{I.P.}}{kTe}} \ell_{eo}^1 \tag{6}$$

The quantity $E_{I.P.}$ is the ionization potential of the metal atom in volts. Using equation (6) in equation (5) yields the following result,

$$\frac{dn_1}{dt} = P_e^1 + P_{rad}^1 + n_e \ell_{eo}^1 \left[n_o - n_e n_1 \mathcal{K}_{el}^o\right] \tag{7}$$

where

$$\mathcal{K}_{el}^o = \frac{g_0}{2g_1}\left(\frac{h^2}{2\pi m_e kT_e}\right)^{3/2} e^{\frac{qE_{I.P.}}{kT_e}} \tag{8}$$

C. Continuity Equation for Metal Atom Ground State

The continuity equation for the ground state of the metal atom includes the effect of both charge exchange and electron collisional ionization.

$$\frac{dn_0}{dt} = -n_A n_o \sum_r \ell_{Ao}^r - n_e \ell_{eo}^1 \left[n_o - n_e n_1 \mathcal{K}_{el}^o\right] \tag{9}$$

The first term in equation (9) is the sum of all the charge exchange rates (eq. (A9)) for levels of the metal ion that have a resonance with the inert gas ions. The second term is the net rate for electron collisional ionization.

D. Continuity Equation for Ground State of Inert Gas

The only loss mechanism for density considered for the inert gas ions was charge exchange. As a result the inert gas ion continuity equation is the following.

$$\frac{dn_A}{dt} = -n_A n_o \sum_r \ell_{Ao}^r \tag{10}$$

E. Charge Neutrality and Electron Energy Equation

Finally, we assume that charge neutrality exists so that the electron number density must balance the total ion density. Therefore,

$$n_e = n_A + \sum_{i=1}^{N} n_i \tag{11}$$

To complete the system of equations an electron energy equation is required. In Chapter 7 of reference 12 flow equations for general reactive systems are developed based on the Bhatnagar-Gross-Krook model for the Boltzmann equation. Based on these results the following electron energy equation was developed in appendix B from equation (56.2) of reference 12.

$$\frac{dT_e}{dt} = -\sum_{j=i+1}^{N} \sum_{i=1}^{N-1} \left\{ \ell_{ei}^j \left[n_i - \frac{q_i}{q_j} n_j e^{\frac{q(E_j-E_i)}{kT_e}} \right] \left[\frac{m_e}{3k} \overline{g_{ei}^2} - T_e \right] \right\}$$

$$- \ell_{eo}^1 \left[n_o - n_e n_1 \mathcal{H}_{el}^o \right] \left[\frac{m_e}{3k} \overline{g_{eo}^2} - T_e \right] \tag{B-5}$$

The term $\overline{g_{ei}^2}$ is the average of the square of the relative velocity between all electrons and all level i particles that take part in exciting level j. Similarly, $\overline{g_{eo}^2}$ is the average square velocity between all electrons and all ground state metal atoms that take part in ionization. The excitation rate of level j as a result of electron collisions with level i is denoted by ℓ_{ei}^j.

The system of equations is now complete. It consists of N - 1 equations for the number density of considered excited levels of the metal ion (eq. (4)), continuity equations for the metal ion ground state number density (eq. (7)), metal atom ground state number density (eq. (9)), inert gas ion number density (eq. (10)), and electron number density (eq. (11)), and finally of the electron temperature (eq. (B-5)). Before a solution can be obtained, however, expressions for the electron excitation rate, ℓ^j_{ei}, electron ionization rate, ℓ^1_{eo}, charge exchange rate, ℓ^r_{Ao}, and the relative velocity terms g^2_{ei} and g^2_{eo} must be known. In the next section expressions for these quantities will be developed.

IV. CROSS SECTIONS AND REACTION RATES

In appendix C the general expressions for the electron excitation and ionization rates (eqs. (C-7) and (C-8)), are developed. The results are in terms of an integral over electron energy, ϕ_e, with the cross section for excitation, S^j_{ei}, or ionization, S_I, appearing in the integrand. To carry out the ϕ_e integrations in equations (C-7) and (C-8) expressions for the cross sections S^j_{ei} and S_I must be known. For ionization by electron collisions of the metals to be considered (Mg, Ca, Sr, and Ba) experimental values of the cross section as functions of electron energy are given in reference 14. From threshhold ($\phi_e = E_{I.P.}$), the cross sections increase rapidly to some maximum and then begin to decrease slowly as ϕ_e increases. Since we will be considering electron temperatures below the value of ϕ_e for maximum cross section, a linear approximation to the initial portion of the S_I versus ϕ_e curve was used to calculate ℓ^1_{eo}.

$$\begin{aligned} S_I &= a^1_{eo}(\phi_e - E_{I.P.}) && \phi_e \geq E_{I.P.} \\ S_I &= 0 && \phi_e \leq E_{I.P.} \end{aligned} \tag{12}$$

The quantity a^1_{eo} is the slope of the initial portion of the S_I versus ϕ_e curve. Substituting equation (12) in (C-8) and integrating results in the following

$$\ell'_{eo} = a'_{eo} \sqrt{\frac{8kT_e}{\pi m_e}} \left[\frac{2kT_e}{q} + E_{I.P.}\right] e^{-\frac{qE_{I.P.}}{kT_e}} \tag{13}$$

In the case of electron excitation the Bohr-Thomson approximation for the cross section was utilized. Experimental values for these cross sections are not available. The Bohr-Thomson approximation used is of the following form (ref. 15).

$$S_{ei}^{j} = 0 \qquad (E_j - E_i) \geq \phi_e$$

$$S_{ei}^{j} = \frac{\sigma_o}{\phi_e}\left(\frac{1}{E_j - E_i} - \frac{1}{\phi_e}\right) \qquad (E_j - E_i) \leq \phi_e \leq (E_{j+1} - E_i)$$

$$S_{ei}^{j} = \frac{\sigma_o}{\phi_e}\left(\frac{1}{E_j - E_i} - \frac{1}{E_{j+1} - E_i}\right) \qquad \phi_e \geq (E_{j+1} - E_i) \qquad (14)$$

The parameter $\sigma_o = 6.513\times10^{-18}\ V^2m^2$ in equation (14). Using equation (14) in (C-7) yields the following result.

$$\ell_{ei}^{j} = 2\sqrt{\frac{2q}{\pi m_e}}\left(\frac{q}{kT_e}\right)^{1/2}\frac{\sigma_o}{(E_j - E_i)}\left(e^{-\frac{q(E_j-E_i)}{kT_e}} - \frac{(E_j - E_i)}{(E_{j+1} - E_i)}e^{-\frac{q(E_{j+1}-E_i)}{kT_e}} - \frac{q(E_j - E_i)}{kT_e}\left\{Ei\left[\frac{q(E_j - E_i)}{kT_e}\right] - Ei\left[\frac{q(E_{j+1} - E_i)}{kT_e}\right]\right\}\right) \qquad (15)$$

The term Ei(x) is the exponential integral.

$$Ei(x) = \int_x^{\infty} \frac{e^{-u}}{u}\,du \qquad (16)$$

Equations (13) and (15) give the electron inelastic collision rates utilized in the solution. Since the Bohr-Thomson cross section for electron excitation is usually larger than the actual cross section (ref. 15), we are overestimating the effect of electron collisions in the production of excited states of the metal ion. Similarly, since our approximation to the ionization cross section is larger than the experimental value we are overestimating the production of ground state metal ions. Overestimating the electron excitation and ionization rates underestimates the possibility of a population inversion by charge exchange. This is so because the electron processes drive the metal ion level densities toward their equilibrium values thus eliminating the inversion.

The calculation of the charge exchange rate, ℓ_{Ao}^{r}, is carried out in appendix D. In making the calculation a linear approximation for the cross section was utilized.

$$S_{Ao}^{r} = a_{Ao}^{r}\phi + b_{Ao}^{r} \qquad (17)$$

Where a_{Ao}^{r} and b_{Ao}^{r} are constants and ϕ is the relative energy,

$$q\phi = \frac{1}{2}\frac{m_A m_o}{m_A + m_o} g^2 \tag{18}$$

Values for a^r_{Ao} and b^r_{Ao} were obtained by fitting equation (17) to the data of references 16 and 17. Since the data is for perfect resonance (A = B, $\Delta E = 0$ in eq. (1)), we will be overestimating the charge exchange rate. From equation (D-6) of appendix B and using the approximation $\frac{kT_A}{m_A} >> \frac{kT_o}{m_o}$ we obtain the following expression for ℓ^r_{Ao}.

$$\ell^r_{Ao} = v\left\{\frac{kT_A m_o}{q(m_o + m_A)} a^r_{Ao}\left[\operatorname{erf} s\left(s^2 + \frac{3}{4}s^{-2} + 3\right) + \frac{e^{-s^2}}{\sqrt{\pi}}\left(s + \frac{5}{2}s^{-1}\right)\right] + b^r_{Ao}\left[\operatorname{erf} s\left(1 + \frac{s^{-2}}{2}\right) + \frac{e^{-s^2}}{\sqrt{\pi}}s^{-1}\right]\right\} \tag{19}$$

Where,

$$s = \frac{v}{\sqrt{\frac{2kT_A}{m_A}}} = \frac{\left|\vec{v}_A - \vec{v}_o\right|}{\sqrt{\frac{2kT_A}{m_A}}} \tag{20}$$

and erf s is the error function defined by equation (D-8). The quantity v will be referred to as the slip velocity since it indicates how fast the inert gas ion beam is "slipping" through the metal atom gas.

The average relative velocity terms $\underline{\underline{g^2_{ei}}}$ and $\underline{\underline{g^2_{eo}}}$ are calculated using equations (B-3a) and (B-3b). Substituting equations (13) and (15) in equation (B-3a) and performing the integration yields the following

$$\frac{m_e}{3k}\underline{\underline{g^2_{ei}}} = \frac{2}{3}T_e\theta_1\left[\frac{q(E_j - E_i)}{kT_e}, \frac{q(E_{j+1} - E_i)}{kT_e}, \frac{E_j - E_i}{E_{j+1} - E_i}\right] \tag{21}$$

Where,

$$\theta_1(x,y,z) = \frac{[2 + x(1 - z) - z]e^{-x} - [1 + y - x]e^{-y}}{e^{-x} - ze^{-y} - x[Ei(x) - Ei(y)]} \tag{22}$$

and Ei is the exponential integral defined by equation (16). Also, if equations (12) and (13) are substituted in equation (B-3b) the following is obtained.

$$\frac{m_e}{3k}\,\overline{g_{eo}^2} = \frac{2}{3}\,T_e\theta_2\left(\frac{qE_{I.P.}}{kTe}\right) \tag{23}$$

Where,

$$\theta_2(x) = \frac{6 + 4x + x^2}{2 + x} \tag{24}$$

Equations (21) and (23) were used in equation (B-5) to complete the electron energy equation.

V. MODEL FOR METAL ION

There are many possible metal-inert gas systems where charge exchange may produce an inversion. However, the only system that is numerically evaluated in this study is calcium-xenon. A model of the calcium ion used in the analysis is shown in figure 2. Wavelengths for all the allowed transitions are given in nanometers and were obtained from reference 18. Only the 5s level has a near resonance with xenon ions [$\Delta E = -0.45$ eV in eq. (1)]. As a result charge exchange will populate only the 5s level. This should be an advantage over other systems (refs. 1 to 8) where several levels have near resonances and thus will compete for charge exchange population.

As can be seen in figure 2, the two 4p, 5p, and 4d levels are nearly the same in energy. Using equations (A-3) and (A-6) we can write the net electron collisional excitation rate between two of these adjacent levels as follows,

$$P_{ei}^{j} \equiv n_e \ell_{ei}^{j}\left(n_i - n_j\,\frac{g_i}{g_j}\,e^{\frac{q(E_j-E_i)}{kTe}}\right) \qquad j > i \tag{25}$$

Referring to equation (15) we see that if $E_j \to E_i$ then $\ell_{ei}^{j} \to \infty$. Therefore, in order that the term defined in equation (25) remains finite the following condition must be satisfied.

$$n_i - n_j\,\frac{g_i}{g_j}\,e^{\frac{q(E_j-E_i)}{kTe}} \to 0 \tag{26}$$

Therefore,

$$n_i = n_j\,\frac{g_i}{g_j}\,e^{\frac{q(E_j-E_i)}{kTe}} \approx n_j\,\frac{g_i}{g_j} \tag{27}$$

which is just the Boltzmann equilibrium relation (eq. (A-6)). For the adjacent 4p, 5p, and 4d levels equation (27) was used to relate the densities. As a result the system of equations to be solved consists of $N - L$ differential equations for calcium ion level densities, a differential equation for xenon ion density, a differential equation for calcium atom density, a differential equation for electron temperature, and L algebraic equations for calcium ion level densities. The total number of calcium levels is $N = 8$, and $L = 3$ is the number of pairs of adjacent levels where the approximation given by equation (27) is used.

The transition probabilities for the allowed transitions obtained from reference 19 are presented in table II. Also appearing in table II are the ionization cross section coefficient, a^1_{eo}, and the charge exchange cross section coefficients, a^4_{Ao} and b^4_{Ao}. The superscript 4 refers to the 5s upper laser level. These coefficients were obtained by fitting the data of references 14 and 17. We can expect to find inversions between the 5s level and the two 4p levels. Inversions on these levels would produce lasing at 373.7 nm and 370.6 nm.

VI. RESULTS

A numerical solution of the equations was carried out on an IBM 7094 computer. Numerical approximations to the exponential integral, Ei, appearing in the excitation rate expression (eq. (15)) were obtained from reference 20.

There are two important parameters that result from the calculations. The first is the gain defined as follows,

$$G = \frac{n_u}{g_u} - \frac{n_\ell}{g_\ell} \tag{28}$$

The subscript u denotes the upper laser level and ℓ denotes the lower laser level. For $G > 0$ an inversion exists and the gain coefficient, α, can be calculated using equation (28). For a Doppler broadened line the gain coefficient is given as follows (ref. 21),

$$\alpha = \frac{1}{8\pi^{3/2}} \sqrt{\frac{m_o}{2kT_B}}\, g_u A_u^\ell \lambda^3 G$$

or, in MKS units,

$$\alpha = 1.741\times10^{-4} \sqrt{\frac{M_B}{T_B}}\, g_u A_u^\ell \lambda^3 G \ m^{-1} \tag{29}$$

The term m_o is the mass of an atom of the lasing gas, T_B is the temperature of the lasing gas, g_u is the degeneracy of the upper laser level,

A_u^ℓ is the transition probability for the laser transition, λ is the wavelength of the laser transition, and M_B is the atomic weight of the lasing gas. The value of α for $10^{15} \leq G \leq 10^{16}$ m^{-3} and $T_B = 1$ eV in the calcium-xenon system with $\lambda = 3737A^o$ is $0.15 \leq \alpha \leq 1.5$ m^{-1} and with $\lambda = 3706A^o$, $0.08 \leq \alpha \leq 0.8$.

The second important parameter resulting from the analysis is the inversion time, τ. This has been arbitrarily defined as the length of time the gain, G, remains greater than $10^{14} m^{-3}$. The investigation considered the effect of the initial conditions, $(T_e)_{t=o}$ and $(n_o)_{t=o}$, as well as slip velocity, v, and charge exchange cross section coefficient, b_{Ao}^4, on the gain, G, and inversion time, τ. For all cases investigated so far the xenon ion temperature has been arbitrarily set at $T_{Xe} = 0.1 (T_e)_{t=o}$. Also, the effect of the radiation field has been neglected, $(T_r \to 0)$. Finally, all densities except calcium atom density, n_o, and xenon ion density $(n_{xe})_i$, are zero at $t = 0$.

As mentioned before, inversions can occur between the 5s level and the two 4p levels. Since the densities of the two 4p lower laser levels are related by equation (27) the gain, G, and inversion time, τ, for each of the laser lines will be equal (see eq. (28)).

Figure 3 shows G as a function of time for three different initial electron temperatures. The gain increases to a fairly "flat" maximum and then decreases. For $(T_e)_{t=o} \leq 3$ eV a plateau occurs in the gain vs time curve. However, for large electron temperatures this plateau disappears. We see that the inversion time is sensitive to initial electron temperature while the maximum gain is almost independent of $(T_e)_{t=o}$. These results are as expected. It is the electron temperature that drives the level densities toward their equilibrium values by electron collisional excitation and thus destroys the inversion. Thus, the inversion time should depend strongly on the electron temperature. The maximum gain, however, is directly proportional to the maximum upper laser level density. Since this density depends mainly on the charge exchange mechanism, which is independent of T_e, we do not expect the maximum gain to depend strongly on T_e.

The sensitivity of inversion time, τ, to initial electron temperature is shown in figure 4. We also see that τ is much less sensitive to the initial calcium atom density, $(n_o)_{t=o}$, than to electron temperature. An electron temperature, $(T_e)_{t=o} = 0.7$ eV, was the smallest value used in the calculations. Although τ appears to be increasing as $T_e \to 0$, we expect this trend to reverse for very small electron temperatures. As $T_e \to 0$, the deexcitation rate, $k_{ei} \to \infty$. Therefore, the upper laser level will be collisionally deexcited so fast that an inversion will not have time to form and $\tau \to 0$. A complete explanation for the minimum that occurs near $(T_e)_{t=o} = 1.5$ eV has not been found as yet. This minimum disappears as $(n_o)_{t=o}$ is decreased. The inversion time decreases rapidly from $(T_e)_{t=o} \approx 2$ eV to $(T_e)_{t=o} \approx 5$ eV. Then the decrease is much slower and appears to approach an asymptote of about 10^{-8} second. Figure 5 shows the dependency of τ on the initial calcium

atom density, $(n_o)_{t=o}$. An increase of 10^{19} to 10^{21} in $(n_o)_{t=o}$ decreases the inversion time by a factor of approximately 10.

The maximum gain, G_{max}, depends strongly on the initial calcium atom density, $(n_o)_{t=o}$. Figure 6 shows this dependence. As mentioned earlier, the maximum gain depends on the charge exchange mechanism. From equation (A-9) we see that the charge exchange production term depends linearly on n_o, n_{xe}, and ℓ^4_{Ao}. As a result we expect a strong dependence of G_{max} on these quantities. Since the slip velocity, v, is greater than the xenon ion thermal speed, $\sqrt{2kT_{Xe}/m_{Xe}}$, the charge exchange rate, ℓ^4_{Ao}, can be approximated by equation (D-9). Therefore, ℓ^4_{Ao} is directly proportional to v. And since a^4_{Ao} is small, ℓ^4_{Ao} is also directly proportional to b^4_{Ao}. Therefore, changing either $(n_o)_{t=o}$, $(n_{xe})_{t=o}$, v, or b^4_{Ao} will produce the same effect on the maximum gain. Figure 7 demonstrates this conclusion. A change of a factor of 10 in either $(n_o)_{t=o}$ or v produces nearly the same change in G_{max}. A plot of G_{max} vs b^4_{Ao} or G_{max} vs $(n_{xe})_{t=o}$ would show results similar to those of figure 6 or 7.

Although not shown in this report, the analysis predicted the following results for electron temperature. For $(T_e)_{t=o} < 5eV$ the electron temperature remains nearly constant with time. At $(T_e)_{t=o} = 5eV$ the temperature decreases by less than 5 percent for the time interval $0 \leq t \leq \tau$. For larger initial electron temperatures the decrease becomes significant. When $(T_e)_{t=o} = 20$ eV the electron temperature decreases by 25 percent for the time interval $0 \leq t \leq \tau$.

VI. CONCLUDING REMARKS

Results obtained for the calcium-xenon charge exchange system indicate maximum gains of 10^{15}-10^{17} m^{-3} with inversion times of 2×10^{-8} - 8×10^{-7} second. In obtaining these results the effect of the radiation field (stimulated emission) has been ignored. Including the radiation will certainly reduce the gain.

The inversion time, τ, is determined mainly by the electron collisional processes and thus by the electron temperature. For electron temperatures greater than 2eV, τ decreases rapidly. Maximum gain, G_{max}, however, is nearly independent of electron temperature and depends mainly on the charge exchange mechanism. As a result, increasing either the initial xenon ion density, initial calcium atom density, slip velocity, or charge exchange cross section will yield the same increase in the maximum gain.

As pointed out previously, we are overestimating the charge exchange rate by using the resonant cross section to approximate the near resonant case. Therefore, the results for maximum gain are optimistic. Also, however, the Bohr-Thomson cross section used overestimates the electron excitation processes. As a result the inversion times calculated in the analysis are underestimates of actual inversion times.

Consider how the results apply to the MPD arc system described in figure 1. As mentioned in the Introduction, the model used should approximate only the initial interaction between the xenon ion beam and the neutral calcium gas cloud. An estimate of the length of the initial interaction for $G > 10^{14}\ m^{-3}$ is given by the product of the inversion time, τ, and the slip velocity, v. Therefore, from the results we expect the initial interaction to have lengths the order of 0.05 - 1 cm. The inversion will not necessarily disappear after this initial interaction in the actual system, however. Since the xenon ion beam will continue to penetrate into the calcium cloud, we would expect the inversion to be maintained until the calcium cloud is completely penetrated by the xenon ion beam. The gain, however, will be less than the gains calculated for the initial interaction region.

APPENDIX A - DEVELOPMENT OF PRODUCTION TERMS FOR iTH LEVEL CONTINUITY EQUATION

1. Collisional Electron Excitation

Population of the ith level occurs as a result of both collisional and radiative effects. We consider two possible collisional mechanisms for exciting the ith level; electron collisions

$$e + B_j^+ \underset{k_{ei}^j}{\overset{\ell_{ej}^i}{\rightleftharpoons}} e + B_i^+ \qquad \text{(A-1)}$$

and if the level is near resonant then charge exchange described by equation (1a) is also important. In equation (A-1) ℓ_{ej}^i is the electron collisional excitation rate of the ith level from the jth level and k_{ei}^j is the corresponding deexcitation rate from i to j, (i > j).

The contribution to the density of the ith level from the reaction described by equation (A-1) is the following (ref. 12, p. 264).

$$n_e n_j \ell_{ej}^i - n_e n_i k_{ei}^j \qquad i > j \qquad \text{(A-2)}$$

where n denotes density and the subscript e denotes electrons. Term (A-2) gives the contribution to the ith level from lower levels (i > j). Similarly, the ith level contributes to the density of all levels above the ith.

$$-\left(n_e n_i \ell_{ei}^j - n_e n_i k_{ej}^i\right) \qquad j > i \qquad \text{(A-3)}$$

Term (A-3) gives the loss rate of the ith level due to excitation of a level j above the ith level, (j > i). Therefore, the net production of the ith level due to electron excitation is the following.

$$P_e^i = \sum_{j=1}^{i-1} \left(n_e n_j \ell_{ej}^i - n_e n_i k_{ei}^j\right) - \sum_{j=i+1}^{N} \left(n_e n_i \ell_{ei}^j - n_e n_j k_{ej}^i\right) \qquad \text{(A-4)}$$

Where N is the total number of excited levels considered. (The ground state of the metal ion is denoted by i = 1.)

If equilibrium conditions exist then the production rate terms must vanish. For example, equation (A-2) set equal to zero yields the following

$$k_{ei}^{j}\Big|_{eq.} = \ell_{ej}^{i}\Big|_{eq.} \left(\frac{n_j}{n_i}\right)_{eq.} \tag{A-5}$$

At equilibrium the densities obey the Boltzmann relation (ref. 13, p. 63).

$$\left(\frac{n_j}{n_i}\right)_{eq.} = \frac{g_j}{g_i} e^{-\frac{q(E_j-E_i)}{kT_e}} \tag{A-6}$$

Where g denotes degeneracy, E is the energy of a given level in eV, q is the magnitude of the electron charge (1.6×10^{-19} coulombs), and k is the Boltzmann constant (1.38×10^{-23} joule/^{o}K). If we substitute equation (A-6) in equation (A-5) the following is obtained.

$$k_{ei}^{j}\Big|_{eq.} = \ell_{ej}^{i}\Big|_{eq.} \frac{g_j}{g_i} e^{-\frac{q(E_j-E_i)}{kT_e}} \tag{A-7}$$

Using the usual assumption that equation (A-7) holds away from equilibrium we can replace k_{ei}^{j} and k_{ej}^{i} in equation (A-4) by equation (A-7). Therefore we get the following.

$$P_e^i = n_e \left[\sum_{j=1}^{i-1} n_j \ell_{ej}^{i} - \frac{e^{\frac{qE_i}{kT_e}}}{g_i} n_i \sum_{j=1}^{i-1} \ell_{ej}^{i} g_j e^{-\frac{qE_j}{kT_e}} \right.$$

$$\left. - n_i \sum_{j=i+1}^{N} \ell_{ei}^{j} + g_i e^{-\frac{qE_i}{kT_e}} \sum_{j=i+1}^{N} \frac{n_j}{g_j} \ell_{ei}^{j} e^{\frac{qE_j}{kT_e}} \right] \tag{A-8}$$

Equation (A-8) gives the production rate for the ith level as a result of collisional electron excitation.

2. Charge Exchange Excitation

If the ith level is in resonance or near resonance with the inert gas ion, then charge exchange will also contribute to the production of the ith level.

$$P_A^i = n_A n_o \ell_{Ao}^i \delta_{ri} \tag{A-9}$$

Where n_A is the density of the inert gas ions and n_o is the density of the ground state of the metal atom. The subscript r denotes a level in resonance or near resonance with the inert gas and $\delta_{ri} = 0$ if $r \neq i$ or $\delta_{ri} = 1$ if $r = i$.

3. Spontaneous and Stimulated Emission

Radiation effects contribute to the density of the ith level by way of spontaneous emission and stimulated emission and absorption. The net contribution from radiation is given as follows (ref. 12, p. 320)

$$P_{rad}^i = \sum_{j=1}^{i-1} \left[n_j B_j^i \phi(\nu_i^j) - n_k B_k^j \phi(\nu_j^i) - n_i A_i^j \right]$$

$$+ \sum_{j=i+1}^{N} \left[- n_i B_i^j \phi(\nu_j^i) + n_j B_j^i \phi(\nu_i^j) + n_j A_j^i \right] \tag{A-10}$$

The term A_i^j is the spontaneous emission coefficient (or transition probability) with the units of sec^{-1} for spontaneous emission from the ith level to the jth level. The stimulated emission or absorption coefficient for stimulated emission or absorption from the ith level to the jth level is denoted by B_i^j. It has units m^2/joule sec. The radiation field energy flux per frequency interval (joule/m^2) is given by $\phi(\nu_i^j)$ where

$$h\nu_i^j = q(E_j - E_i) = q\left|E_i - E_j\right| \tag{A-11}$$

The first sum in equation (A-10) gives the radiation contribution to the ith level from all levels below i. The first term in the sum being stimulated absorption where a lower level is converted to the ith level, the second term is stimulated emission where the ith level drops to a lower level, and the last term is spontaneous emission where the ith level drops to a lower level. The last sum in equation (A-10) gives the radiation contribution to the ith level from all levels above i. Each term has a meaning similar to those in the first sum except that i now replaces j as the lower level.

For an accurate solution to the problem the radiation field energy flux, $\phi(\nu)$, should be coupled to the densities of all species through a

radiative transfer equation. However, to simplify the problem the following form for $\phi(\nu)$ was assumed.

$$\phi(\nu_i^j) = \frac{2h\nu_i^{j\,3}}{c^2}\left(e^{\frac{h\nu_i^j}{kT_r}} - 1\right)^{-1}(1 + \gamma\delta_{uj}\delta_{\ell i}) \qquad \text{(A-12)}$$

In equation (A-12) c is the speed of light and $\delta_{ij} = 0$ for $i \neq j$ and $\delta_{ij} = 1$ for $i = j$. The subscripts u and ℓ denote levels where a population inversion exists. Thus, u represents the upper level and ℓ the lower level of the inversion. In choosing equation (A-12) for $\phi(\nu)$ we are assuming the radiation field has a Planck distribution ref. 13, p. 721) in frequency and can be characterized by some radiation temperature, T_r (ref. 12, p. 320). In addition, the Planck distribution has been multiplied by the factor $(1 + \gamma\delta_{uj}\delta_{\ell i})$ where γ is a constant. This factor is added to account for an increase in radiation energy density that will result if lasing occurs on the transition $u \to \ell$. Both γ and T_r are treated as constants in the analysis.

To simplify equation (A-10) we use equation (A-12) for $\phi(\nu)$ and the Einstein relations (ref. 13, p. 722),

$$B_j^i = \frac{g_i}{g_j}B_i^j \qquad B_j^i = \frac{c^2}{2h\nu_i^{j\,3}}A_j^i \qquad (j > i) \qquad \text{(A-13)}$$

where g_i is the degeneracy of the ith level. Using equations (A-11), (A-12), and (A-13) in equation (A-10) yields the following result.

$$P_{rad}^i = \sum_{j=i+1}^{N} n_j A_j + \sum_{j=i+1}^{N} \frac{n_j A_j^i(1 + \gamma\delta_{uj}\delta_{\ell i})}{\exp[q(E_j - E_i)/kT_r] - 1}$$

$$+ g_i \sum_{j=1}^{i-1} \frac{n_j A_i^j(1 + \gamma\delta_{ui}\delta_{\ell j})}{g_j\{\exp[q(E_i - E_j)/kT_r] - 1\}} - n_i\left\{\sum_{j=1}^{i-1} A_i^j\right.$$

$$\left. + \sum_{j=1}^{i-1} \frac{A_i^j(1 + \gamma\delta_{ui}\delta_{\ell j})}{\exp[q(E_i - E_j)/kT_r] - 1} + \frac{1}{g_i}\sum_{j=i+1}^{N} \frac{g_j A_j^i(1 + \gamma\delta_{uj}\delta_{\ell i})}{\exp[q(E_j - E_i)/kT_r] - 1}\right\} \qquad \text{(A-14)}$$

Equation (A-14) gives the production rate of the ith level by spontaneous emission and stimulated emission and absorption.

APPENDIX B - ELECTRON ENERGY EQUATION

From equation (56.2) of reference 12 we obtain the following electron energy equation.

$$\frac{3}{2} n_e k \frac{dT_e}{dt} = \frac{3}{2} n_e k \left[\frac{\partial T_e}{\partial t} + \vec{v}_e \cdot \nabla T_e\right] = \sum_s K_{es} \left[\frac{3k(T_s - T_e)}{m_s}\right]$$

$$-n_e \sum_{j=i+1}^{N} \sum_{i=1}^{N-1} \ell_{ei}^{j} \left[n_i - \frac{g_i}{g_j} n_j e^{\frac{q(E_j - E_i)}{kT_e}}\right] \left[\frac{m_e}{2} \llcorner g_{ei}^2 \lrcorner - \frac{3}{2} kT_e\right]$$

$$- n_e \ell'_{eo} \left[n_o - n_e n_1 \chi_{e1}^{o}\right] \frac{m_e}{2} \llcorner g_{eo}^2 \lrcorner - \frac{3}{2} kT_e \qquad \text{(B-1)}$$

Where, the first term on the right-hand side of equation (B-1) is the elastic electron collisional energy transfer rate. The second term is the energy transfer rate due to electron excitation collisions of the metal ion, (eq. (A-1)). And the third term is the energy transfer rate resulting from electron collisional ionization of neutral metal atoms. Other terms appearing in equation (B-1) are the following.

$$K_{es} = \frac{4}{3} m_e n_e n_s \sqrt{\frac{8kT_e}{\pi m_e}} \sigma_{es} \qquad \text{(B-2a)}$$

$$\sigma_{es} = \frac{1}{2} \left(\frac{q}{kT_e}\right)^3 \int_0^\infty \sigma_{es}^{m} \phi_e^2 e^{-\frac{q\phi_e}{kT_e}} d\phi_e \qquad \text{(B-2b)}$$

$$\ell_{ei}^{j} \llcorner g_{ei}^2 \lrcorner = \frac{8}{\sqrt{2\pi}} \left(\frac{q}{m_e}\right)^{3/2} \left(\frac{q}{kT_e}\right)^{3/2} \int_0^\infty S_{ei}^{j} \phi_e^2 e^{-\frac{q\phi_e}{kT_e}} d\phi_e \qquad \text{(B-3a)}$$

$$\ell'_{eo} \llcorner g_{eo}^2 \lrcorner = \frac{8}{\sqrt{2\pi}} \left(\frac{q}{m_e}\right)^{3/2} \left(\frac{q}{kT_e}\right)^{3/2} \int_0^\infty S_i \phi_e^2 e^{\frac{q\phi_e}{kT_e}} d\phi_e \qquad \text{(B-3b)}$$

Definitions of these terms are obtained from reference 12. Three cross sections appear in equations (B-2b) and (B-3b). They are the elastic momentum transfer cross section, σ_{es}^{m}, for collisions between electrons and species s, the inelastic excitation cross section, S_{ei}^{j}, for production of level j due to collisions between electrons and level i, and the electron ionization cross section, S_I, for the metal atom. All of these quantities are functions of electron energy, ϕ_e. The term, $\llcorner g_{ei}^2 \lrcorner$, is the average of the square of the relative velocity between the electrons and level i particles that take part in excitation of level j. Also, $\llcorner g_{eo}^2 \lrcorner$ is a similar average square velocity for electrons and neutral metal atoms that take part in ionization. At equilibrium the following condition holds for a reaction like that described by equation (A-1).

$$\frac{m_e}{2} \llcorner g_{ei}^2 \lrcorner = \frac{m_e}{2} \llcorner g_{ej}^2 \lrcorner + (E_j - E_i) \qquad \text{(B-4a)}$$

Also, at equilibrium

$$\frac{m_e}{2} \llcorner g_{eo}^2 \lrcorner = \frac{m_e}{2} \llcorner g_{el}^2 \lrcorner + E_{I.P.} \qquad \text{(B-4b)}$$

The quantity $(E_j - E_i)$ is the energy required to produce level j by excitation of level i and $\llcorner g_{ej}^2 \lrcorner$ is the average of the square of the relative velocity between the electrons and level j that result from the excitation reactions. The ionization potential of the metal atom is $E_{I.P.}$ and $\llcorner g_{el}^2 \lrcorner$ is the average square relative velocity between electrons and ground state metal ions that result from ionization. In obtaining equations (B-1) through (B-3) the following approximations were made.

1. $m_e + m_t \approx m_t$, $\therefore \frac{kT_e}{m_e} >> \frac{kT_t}{m_t}$

2. $kT_e >> m_t v_t^2$ (v_t is average velocity of species t)

3. Equations (B-4a) and (B-4b)

4. Heat conduction negligible

5. Velocity gradients negligible

Referring to equation (B-2a) we see that the elastic transfer rates (first term on right-hand side) will be proportional to the mass ratio, m_e/m_s. Since the mass ratio is small the elastic energy transfer rate was neglected. As a result equation (B-1) becomes the following

$$\frac{dT_e}{dt} = - \sum_{j=i+1}^{N} \sum_{i=1}^{N-1} \left\{ \ell_{ei}^{j} \left[n_i - \frac{g_i}{g_j} n_j e^{\frac{q(E_j - E_i)}{kT_e}} \right] \left[\frac{m_e}{3k} \bar{g}_{ei}^{2} - T_e \right] \right\}$$

$$- \ell_{eo}^{1} \left[n_o - n_e n_1 K_{e1}^{o} \right] \left[\frac{m_e}{3k} \bar{g}_{eo}^{2} - T_e \right] \qquad \text{(B-5)}$$

APPENDIX C - ELECTRON EXCITATION AND IONIZATION RATES

A general expression for the production rate of species r as a result of collisions between species s and t based on the Bhatnagar-Gross-Krook model for the Boltzmann equation is given in reference 12 (p. 267-268),

$$\ell_{st}^{r} = \frac{e^{-\frac{v^2}{\alpha^2}}}{\pi^{3/2}\alpha^3} \int_{g=0}^{\infty} \int_{\theta=0}^{\pi} \int_{\phi=0}^{2\pi} g^3 S_{st}^{r}(g) \exp\left[-\frac{g^2}{\alpha^2} + \frac{2gv\cos\theta}{\alpha^2}\right] \sin\theta \, d\theta \, d\phi \, dg \tag{C-1}$$

Terms appearing in equation (C-1) are the following

$$v = |\vec{v}_t - \vec{v}_s| \quad \text{- relative average velocity} \tag{C-2}$$

$$g = |\vec{c}_t - \vec{c}_s| \quad \text{- relative velocity between colliding pair of particles} \tag{C-3}$$

$$\alpha^2 = \frac{2kT_s}{m_s} + \frac{2kT_t}{m_t} \tag{C-4}$$

The cross section for the reaction, S_{st}^{r}, is a function of the relative velocity, g, only. As a result the angular integrations in equation (C-1) can be performed.

$$\ell_{st}^{r} = \frac{e^{-\frac{v^2}{\alpha^2}}}{v\alpha\sqrt{\pi}} \int_{0}^{\infty} g^2 \left(e^{\frac{2gv}{\alpha^2}} - e^{-\frac{2gv}{\alpha^2}}\right) e^{-\frac{g^2}{\alpha^2}} S_{st}^{r} \, dg \tag{C-5}$$

Consider equation (C-5) for electron excitation or ionization collisions. In this case,

$$\frac{kT_e}{m_e} >> \frac{kT_t}{m_t}$$

and

$$\frac{v}{\alpha} \approx \frac{v}{\sqrt{\frac{2kT_e}{m_e}}} << 1$$

As a result the exponential terms in equation (C-5) can be approximated by

$$e^{\frac{2gv}{\alpha^2}} - e^{-\frac{2gv}{\alpha^2}} \approx 2\left(\frac{2gv}{\alpha^2}\right) \qquad \text{(C-6)}$$

Using equation (C-6) in (C-5) and also changing variables from g to electron energy $q\phi_e = \frac{1}{2} m_e g^2$ yields the following results for excitation and ionization.

$$\ell_{ei}^{j} = \frac{8}{\sqrt{\pi}} \left(\frac{q}{2kT_e}\right)^{3/2} \left(\frac{q}{m_e}\right)^{1/2} \int_0^\infty \phi_e S_{ei}^{j} e^{-\frac{q\phi_e}{kT_e}} d\phi_e \qquad \text{(C-7)}$$

$$\ell_{eo}^{i} = \frac{8}{\sqrt{\pi}} \left(\frac{q}{2kT_e}\right)^{3/2} \left(\frac{q}{m_e}\right)^{1/2} \int_0^\infty \phi_e S_I e^{\frac{q\phi_e}{kT_e}} d\phi_e \qquad \text{(C-8)}$$

APPENDIX D - CHARGE EXCHANGE RATE

We begin the calculation of the charge exchange rate by rewriting the general rate equation (eq. (C-5)) in the following manner.

$$\ell^r_{Ao} = \frac{1}{\alpha v\sqrt{\pi}}\left[\int_0^\infty g^2 e^{-\frac{(v-g)^2}{\alpha^2}} S^r_{Ao}\,dg - \int_0^\infty g^2 e^{-\frac{(v+g)^2}{\alpha^2}} S^r_{Ao}\,dg\right] \qquad \text{(D-1)}$$

Now make the following variable changes. In the first integral let $y = v - g$ and in the second integral let $y = v + g$. Also, use the condition that $S^r_{Ao}(g) = S^r_{Ao}(-g)$, since it is a function of relative energy, $\frac{1}{2}\frac{m_A m_o}{m_A + m_o} g^2$.

$$\ell^r_{Ao} = \frac{1}{\alpha\sqrt{\pi}}\left\{ v\left[\int_{-\infty}^\infty S^r_{Ao} e^{-\frac{y^2}{\alpha^2}}\,dy - 2\int_v^\infty S^r_{Ao} e^{-\frac{y^2}{\alpha^2}}\,dy\right]\right.$$

$$+ \frac{1}{v}\left[\int_{-\infty}^\infty S^r_{Ao} y^2 e^{-\frac{y^2}{\alpha^2}}\,dy - 2\int_v^\infty S^r_{Ao} y^2 e^{-\frac{y^2}{\alpha^2}}\,dy\right]$$

$$\left. - 2\left[\int_{-\infty}^\infty S^r_{Ao} y e^{-\frac{y^2}{\alpha^2}}\,dy - 2\int_v^\infty S^r_{Ao} y e^{-\frac{y^2}{\alpha^2}}\,dy\right]\right\} \qquad \text{(D-2)}$$

To proceed further an expression for the cross section, S^r_{Ao} must be known. As pointed out in the Cross Sections and Reaction Rates section, a linear approximation was used for S^r_{Ao}. From equations (17) and (18)

$$S^r_{Ao} = a^r_{Ao}\frac{1}{2q}\mu g^2 + b^r_{Ao}$$

where the reduced mass is given by

$$\mu = \frac{m_A m_o}{m_A + m_o} \tag{D-4}$$

In obtaining equation (D-2) we have used a change of variables such that $g^2 = y^2 - 2yv = v^2$. As a result, the cross section to be used in equation (D-2) has the following form.

$$S^r_{Ao} = a^r_{Ao} \frac{\mu}{2q} (y^2 - 2vy + v^2) + b^r_{Ao} \tag{D-5}$$

Substituting equation (D-5) in (D-2) and integrating yields the following result.

$$\ell^r_{Ao} = v\left\{\frac{\mu\alpha^2}{2q} a^r_{Ao}\left[\text{erf } S\left(S^2 + \frac{3}{4}S^{-2} + 3\right) + \frac{e^{-S^2}}{\sqrt{\pi}}\left(S + \frac{5}{2}S^{-1}\right)\right] + b^r_{Ao}\left[\text{erf } S\left(1 + \frac{S^{-2}}{2}\right) + \frac{e^{-S^2}}{\sqrt{\pi}} S^{-1}\right]\right\} \tag{D-6}$$

Where,

$$S = \frac{v}{\alpha} = \frac{|\vec{v}_A - \vec{v}_o|}{\sqrt{\frac{2kT_A}{m_A} + \frac{2kT_o}{m_o}}} \tag{D-7}$$

and

$$\text{erf } S = \frac{2}{\sqrt{\pi}} \int_0^S e^{-x^2} dx \tag{D-8}$$

It is interesting to look at two limiting cases for equation (D-6). When the difference in average velocities, v, is large compared to the average thermal speed, α, then $S \to \infty$ and equation (D-6) becomes the following.

$$\ell_{Ao}^{r} = |\vec{v}_A - \vec{v}_o| \left[\frac{\mu}{2q} |\vec{v}_A - \vec{v}_o|^2 a_{Ao}^{r} + b_{Ao}^{r} \right], \qquad |\vec{v}_A - \vec{v}_o| >> \sqrt{\frac{2kT_A}{m_A} + \frac{2kT_o}{m_o}} \tag{D-9}$$

When $\alpha >> v$, equation (D-6) becomes the following.

$$\ell_{Ao}^{r} = \sqrt{\frac{8k(T_A m_o + T_o m_A)}{\pi (m_A + m_o)}} \left[\frac{2k(T_A m_o + T_o m_A)}{q(m_A + m_o)} a_{Ao}^{r} + b_{Ao}^{r} \right],$$

$$|\vec{v}_A - \vec{v}_o| << \sqrt{\frac{2kT_A}{m_A} + \frac{2kT_o}{m_o}} \tag{D-10}$$

For the case $S \to \infty$, the charge exchange rate is directly proportional to the difference in average velocities. When $S \to 0$, the charge exchange rate is directly proportional to the average thermal speed.

TABLE I - POSSIBLE CHARGE EXCHANGE LASER SYSTEMS

Upper Laser Level Pumping Reaction	Laser Transition	Laser Wavelength, λ, nm	Energy defect, ΔE, eV	Efficiency, $hc/\lambda I.P._A$
$Xe^+ + Ca \rightarrow Xe + (Ca^+)_u$	$5s^2S_{1/2} \rightarrow 4p^2P_{1/2}$	370.6	-0.451	0.27
	$5s^2S_{1/2} \rightarrow 4p^2P_{3/2}$	373.7	-0.451	0.27
$Xe^+ + Mg \rightarrow Xe + (Mg^+)_u$	$3p^2P_{1/2} \rightarrow 3s^2S_{1/2}$	280.3	0.0615	0.36
	$3p^2P_{3/2} \rightarrow 3s^2S_{1/2}$	279.5	0.0501	0.36
$Xe^+ + Sr \rightarrow Xe + (Sr^+)_u$	$5d^2D_{5/2} \rightarrow 5p^2P_{3/2}$	346.4	-0.182	0.29
	$5d^2D_{3/2} \rightarrow 5p^2P_{3/2}$	347.5	-0.17	0.29
	$5d^2D_{3/2} \rightarrow 5p^2P_{1/2}$	338.1	-0.17	0.30
$Xe^+ + Ba \rightarrow Xe + (Ba^+)_u$	$5f^2F_{5/2} \rightarrow 6d^2D_{5/2}$	889.6	-0.197	0.11
	$5f^2F_{3/2} \rightarrow 6d^2D_{3/2}$	873.4	-0.197	0.11
	$5f^2F_{7/2} \rightarrow 6d^2D_{5/2}$	870.9	-0.227	0.11
$Ar^+ + Mg \rightarrow Ar + (Mg^+)_u$	$4s^2S_{1/2} \rightarrow 3p^2P_{1/2}$	292.9	-0.542	0.27
	$4s^2S_{1/2} \rightarrow 3p^2P_{3/2}$	293.6	-0.542	0.27
$N^+ + Ca \rightarrow N + (Ca^+)_u$	$4f^2F_{7/2} \rightarrow 4d^2D_{5/2}$	892.7	-0.002	0.09
	$4f^2F_{5/2} \rightarrow 4d^2D_{3/2}$	891.2	-0.002	0.09

TABLE II - PARAMETERS FOR CALCIUM MODEL ION

State	Level L	Energy, E_L, eV	Degeneracy, g_L	Radiative Transition Probability, $A_K^L \times 10^{-6}$, sec							
				K = 1	K = 2	K = 3	K = 4	K = 5	K = 6	K = 7	K = 8
$4s^2S_{1/2}$	1	0	2		137	143					
$4p^2P_{1/2}$	2	3.123	2				76.7	311			
$4p^2P_{3/2}$	3	3.151	4				149	61.0	369		
$5s^2S_{1/2}$	4	6.467	2							22.5	23.1
$4d^2D_{3/2}$	5	7.046	4							2.72	0.287
$4d^2D_{5/2}$	6	7.049	6								2.54
$5p^2P_{1/2}$	7	7.505	2								
$5p^2P_{3/2}$	8	7.514	4								

Ionization cross section coefficient: $a'_{eo} = 0.54 \times 10^{-20}$ m^2/eV

Charge exchange cross section coefficients: $a^4_{Ao} = -2.98 \times 10^{-22}$ m^2/eV

$b^4_{Ao} = 4.2 \times 10^{-19}$ m^2

REFERENCES

1. McGowman, J. W. and Stebbings, R. F.; Appl. Opt. Suppl. on Chem. Lasers, 68 (1965).

2. Jensen, R. C., Collins, G. J., and Bennett, W. R.; Phys. Rev. Letters, 23, 363 (1969).

3. Collins, G. J., Jensen, R. C., and Bennett, W. R.; Appl. Phys. Letters, 18, 282 (1971).

4. Riseberg, L. A. and Schearer, L. D.; IEEE J. Quantum Electronics, QE-7, 40 (1971).

5. Collins, G. J., Jensen, R. C., and Bennett, W. R.; Appl. Phys. Letters, 19, 125 (1971).

6. Silfvast, W. T. and Klein, M. B.; Appl. Phys. Letters, 17, 400 (1970).

7. Klein, M. B. and Silfvast, W. T.; Appl. Phys. Letters, 18, 482 (1971).

8. Silfvast, W. T. and Klein, M. B.; Appl. Phys. Letters, 20, 501 (1972).

9. Seikel, G. R., Connolly, D. J., Michels, C. J., Richley, E. A., Smith, J. M., and Sovie, R. J.; NASA SP-226 (1970), p. 1.

10. John, R. G.; "Physics of Electric Propulsion," McGraw-Hill, New York, N.Y., 1968, pp. 235-253.

11. Michels, C. J. and Sigman, D. R.; AIAA J. 9, 1144 (1971).

12. Burgers, J. M.; "Flow Equations for Composite Gases," Academic Press, New York, N.Y. (1969).

13. Fowler, R. H.; "Statistical Mechanics," Cambridge University Press, London (1966).

14. Vainshtein, L. A., Ochkur, V. I., Rakhovskii, V. I., and Stepanov, A. M.; Soviet Phys. - JETP, 34, 271 (1972).

15. Ochkur, V. I., and Petrun'kin, A. M.; Opt. Spectrosc., 14, 245 (1963).

16. McDaniel, E. W.; "Collision Phenomena in Ionized Gases," John Wiley & Sons, New York (1964), p. 164.

17. Smirnov, B. M., and Chibisov, M. I.; Soviet Phys. - Tech. Phys., 10, 88 (1965).

18. Striganov, A. R., and Sventitskii, N. S.; "Tables of Spectral Lines of Neutral and Ionized Atoms," Plennum Press, New York (1968).

19. Roberts, T. G. and Hales, W. L.; U.S. Army Missile Command, Redstone Arsenal, RR-TR-62-8 (1962).

20. Abramowitz, M. and Stegun, I. A., eds.; "Handbook of Mathematical Functions with Formulas, Graphs, and Mathematical Tables," NBS Appl. Math. Ser. 55 (1964), p. 231.

21. Lengyel, B. A.; "Lasers," John Wiley & Sons, New York (1971), pp. 12-25.

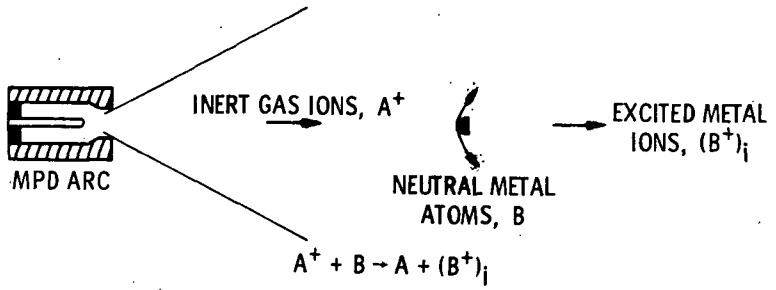

Figure 1. - MPD arc charge exchange laser system.

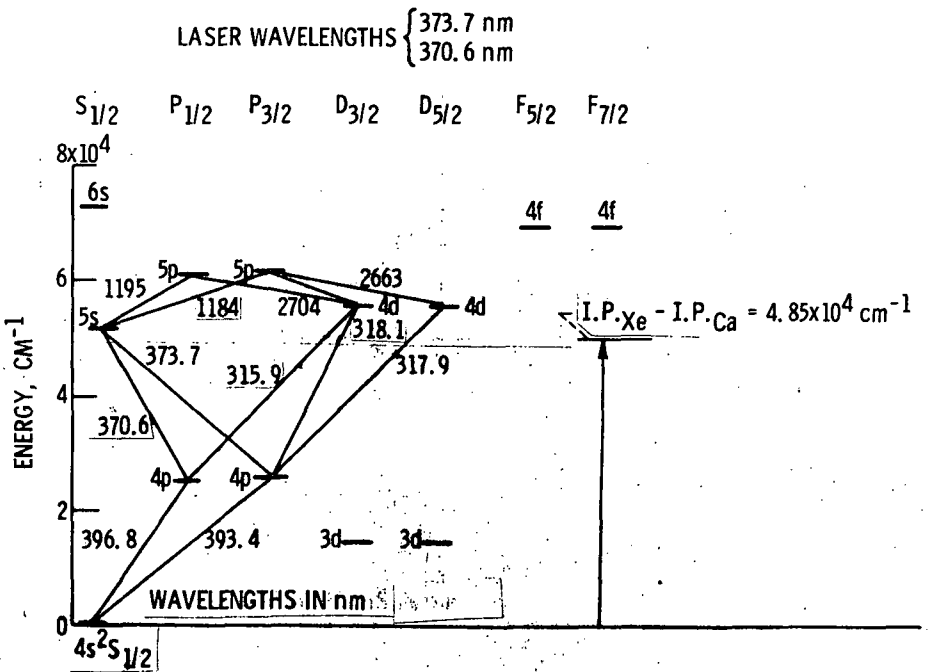

Figure 2. - Energy level diagram of calcium ion.

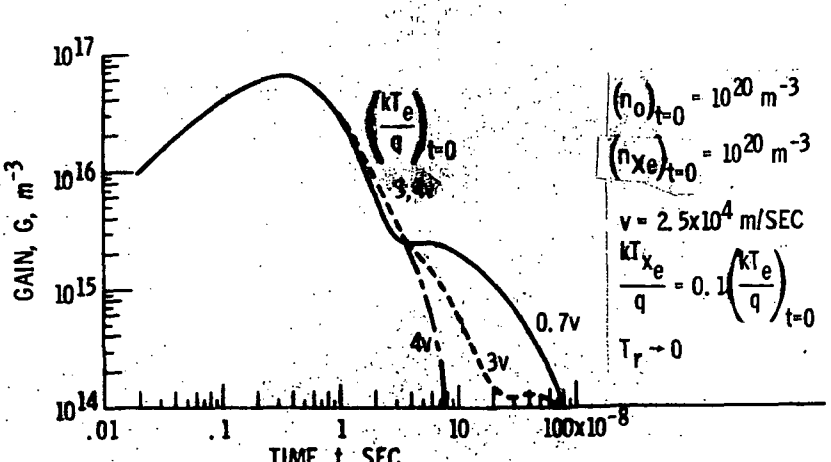

Figure 3. - Gain vs time for Ca-Xe.

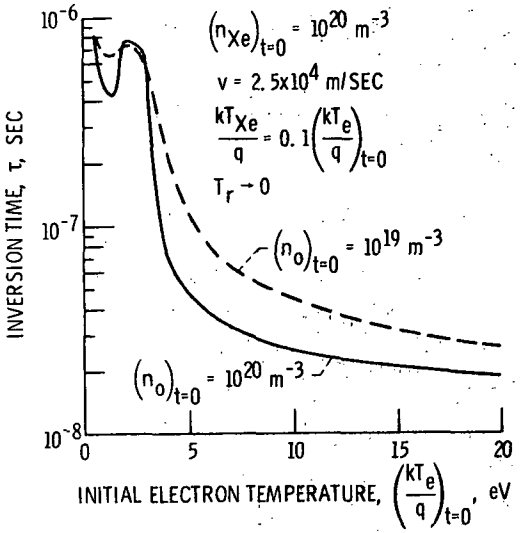

Figure 4. - Inversion time vs initial electron temperature for Ca-Xe.

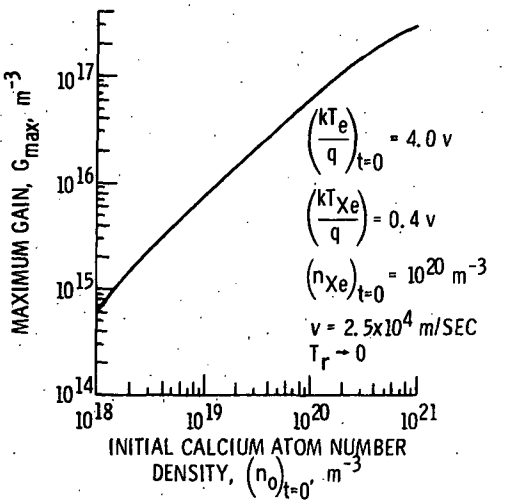

Figure 6. - Maximum gain vs initial calcium number density for Ca-Xe.

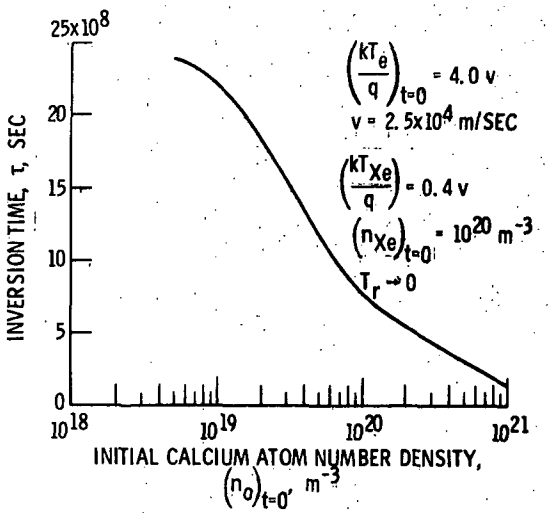

Figure 5. - Inversion time vs initial calcium number density for Ca-Xe.

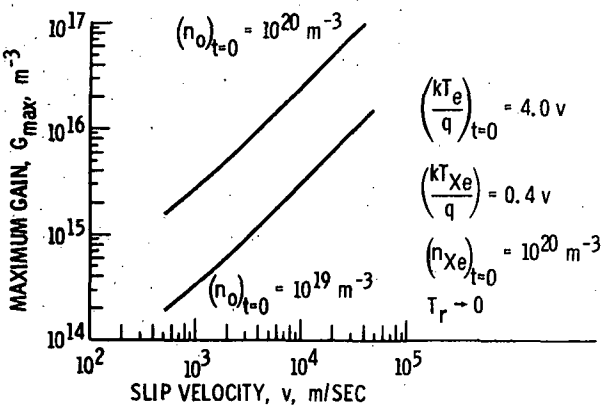

Figure 7. - Maximum gain vs slip velocity for Ca-Xe.